Inductance Calculation Method Considering the Window Effect of Planarized Magnetic Core

Yue Liu, Hongfei Wu, *Senior Member, IEEE*, and Guosheng Ji, *Member, IEEE*

***Abstract*—Inductors with planarized magnetic cores and printed circuit board (PCB) windings are becoming more popular with the development of high-frequency, high-power-density power converters. The magnetic flux distribution in an inductor is affected by the geometry of the magnetic core and windings, which in turn affects the inductance value of the inductor. The accurate inductance calculation method is proposed for PCB-winding planarized inductors. The window effect and shielding effect, which can be recognized as the impact of planarized winding area, PCB winding, and operation frequency on the real inductance of an inductor, are revealed in this article. The impact of the fringing effect, window effect, and shielding effect is analyzed in-depth based on which an improved inductance calculation model is proposed. According to the calculation, finite-element analysis simulation, and experimental tests of various planar inductor samples with different winding turns, frequency, and air gap distance, it is verified that the proposed method is more accurate than previous inductance calculation methods.**

***Index Terms*—Air gaps, fringing effect, inductance calculation, magnetic reluctance, shielding effect, window effect.**

I. Introduction

THERE has been an increasing research interest in searching for higher power density and lower height solutions for power supplies [1], [2]. Due to the rapid development of the wideband-gap semiconductors, the operation frequency of active switches has been increased significantly, which means active devices are no longer the main factor restricting the power density of power converters [3], [4]. On the contrary, the power density of converters is mainly determined by passive magnetics. To solve the above problems, planar magnetics along with printed circuit board (PCB) winding have been developed and proved to be a good candidate to achieve state-of-the-art performance [5], [6]. Usually, the magnetics can be divided into transformers and inductors. The transformer is mainly used for isolation and voltage transformation while the inductor is mainly used for energy storage and filtering. However, whether the transformer or inductor, their inductance values are the most important parameter, which directly affects the operation and performance of the converters [7], [8]. Therefore, the accuracy of the inductance calculation methods is very crucial.

For magnetics without air gaps, because the initial permeability of ferrite is much higher than the air, it is thought that there is no fringing magnetic flux outside the core, and the magnetic line of force is lumped inside the core. The inductance of this kind of magnetics can be calculated by dividing the square of the turns by the magnetic reluctance of the core, which is simple and easy to operate with relatively small errors. However, for magnetics with specific inductance values, due to the high initial permeability of ferrite, the air gap is often employed [9], [10]. Although the magnetic reluctance of the air gap and that of the core is connected in series, the inductance value is mainly determined by the air gap distance. Therefore, the inductance calculation method for magnetics with air gaps has a great effect on the final air gap distance and the height of the magnetics. Especially for planarized magnetics with higher window utilization and lower window height, a slight adjustment of the air gap will affect the winding loss and the total height, thus affecting the overall efficiency and power density [11], [12].

For general calculation methods, inductance values are obtained by calculating the simplified magnetic reluctance of the magnetic core and the air gap. However, the calculation results tend to be smaller than the experimental results because there are actually more closed paths for the magnetic flux. Many works have attributed this problem to the fringing effect of the air gap. In [13], an influence factor for the U-type core and E-type core was introduced to describe the influence of the fringing effect. The influence of the fringing effect is translated into the equivalent parallel magnetic reluctance by introducing some undetermined coefficients in the literature [14], [15]. A method for calculating the magnetic reluctance of air gaps using the Schwarz–Christoffel transformation is proposed and described in [16] and [17]. This method provides the theoretical basis for calculating the influence of the fringing effect, while other methods are only based on experience.

As the magnetic cores develop toward the direction of planarization, the inductance values calculated by the above-mentioned methods are all smaller than the experimental results. The accuracy of the above theoretical calculation methods becomes lower. Hence, for most designers of planar magnetics, finite-element analysis (FEA) simulation has become the most common method to correct the inductance value [18], [19].

Manuscript received 29 March 2023; revised 14 June 2023; accepted 22 July 2023. Date of publication 31 July 2023; date of current version 1 September 2023. This work was supported in part by the National Natural Science Foundation of China under Grants 52122708 and 51977105 and in part by the Natural Science Foundation of Jiangsu Province, China under Grant BK20200017. Recommended for publication by Associate Editor M. Chen. *(Corresponding author: Hongfei Wu.)*

The authors are with the Center for More-Electric-Aircraft Power System, College of Automation Engineering, Nanjing University of Aeronautics and Astronautics, Nanjing 211106, China (e-mail: liuyue0909@nuaa.edu.cn; wuhongfei@nuaa.edu.cn; jiguosheng@nuaa.edu.cn).

Color versions of one or more figures in this article are available at https://doi.org/10.1109/TPEL.2023.3299984.

Digital Object Identifier 10.1109/TPEL.2023.3299984

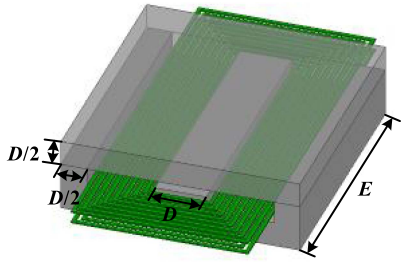

Fig. 1. Planar inductor with PCB winding.

However, the simulation design methods can only be used as a correction tool but cannot be taken into the predesign consideration because it requires a lot of computer resources and time. It is found in this article that the window area of the planarized magnetic core performs as another air gap that cannot be ignored. This phenomenon is defined as the window effect in this article. Further efforts have been spent on the improvement of the inductance calculation method considering the window effect for planar magnetics in order to improve the accuracy.

The rest of this article is organized as follows. In this article, Section II compares the similarities and differences between various inductance calculation methods. The generation mechanism of the window effect and the detailed inductance calculation method when it is taken into consideration are also investigated. In Section III, as the switching frequency increases, the shielding effect of PCB winding is explained and the calculation method is improved by introducing a new permeability coefficient. In Section VI, various planar EI cores with different winding turns, switching frequencies, and air gap distances are calculated, simulated, and tested. Finally, Section V concludes this article.

II. Inductance Calculation Methods Considering Fringing Effect

A. Inductance Calculation With Ideal Flux Distribution (Method A)

According to the definition of the inductance, the flux linkage ψ is generated by the current i flowing through the winding. For inductors with magnetic cores, as shown in Fig. 1, ψ is in direct proportion to i and the ratio is the inductance L as follows:

$$L = \frac{\psi}{i} = \frac{N \cdot \Phi}{i} \tag{1}$$

where N is the turns of winding, and Φ is the magnetic flux.

On the basis of Ampere's loop theorem, the magnetomotive force (MMF) F can be expressed in different forms

$$F = N \cdot i = H \cdot l = \frac{B \cdot l}{\mu} = \frac{\phi}{\mu \cdot A} \cdot l = \phi \cdot R_{\text{total}}. \tag{2}$$

In (2), H is the magnetic field intensity, l is the average magnetic circuit length, B is the magnetic induction intensity, μ is the permeability of the magnetic core, A is the sectional area, and R_{total} is the total magnetic reluctance. By submitting (2) into (1), the calculation expression of the inductance can be rewritten as follows:

$$L = \frac{\psi}{i} = \frac{N \cdot \phi}{\phi \cdot R_{\text{total}}/N} = \frac{N^2}{R_{\text{total}}}. \tag{3}$$

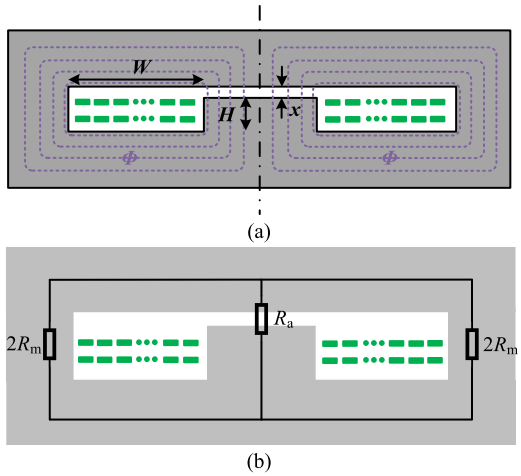

Fig. 2. Sectional view of the planar EI core. (a) Ideal magnetic flux distribution. (b) Simplified magnetic reluctance model.

Based on (3), because the winding turns N is constant, the calculation of the lumped magnetic reluctance R_m is the key point for the final inductance values.

In the engineering applications, to simplify the calculation methods, all magnetic flux is considered to be closed in the magnetic core and the air gap directly above the winding column, as shown in Fig. 2. The magnetic reluctance of the magnetic core R_m and the air gap R_a can be easily described as follows:

$$\begin{cases} R_m = \frac{l_m}{\mu_m \cdot A_m} = \frac{2 \cdot W + 2 \cdot H + x + 2 \cdot D}{\mu_m \cdot D \cdot E} \\ R_a = \frac{l_a}{\mu_a \cdot A_a} = \frac{x}{\mu_a \cdot D \cdot E}. \end{cases} \tag{4}$$

In (4), D, E, and H represent the width, length, and height of the middle winding column. W is the width of the core window and x is the air gap distance. μ_a and μ_m are the permeability of the air and the ferrite used. Then, the inductance calculation method with ideal flux distribution (Method A) can be obtained as follows:

$$L = \frac{N^2}{R_m + R_a}. \tag{5}$$

B. Inductance Calculation Considering the Fringing Effect of Air Gap (Methods B-1, B-2, and B-3)

Although the ideal inductance calculation method in Section II-A is widely used, it is difficult to ensure its accuracy for the inductor case with a large air gap. Since the magnetic flux will diffuse at the air gap, as shown in Fig. 3, which is defined as the fringing effect, the effective cross-sectional area of the air gap ought to be larger and its magnetic reluctance will also decrease accordingly. Hence, many inductance calculation methods considering the fringing effect have been proposed. These methods can be clarified into three categories.

1) Influence Factor Method (Method B-1): The first modified method considering the fringing effect is called the influence

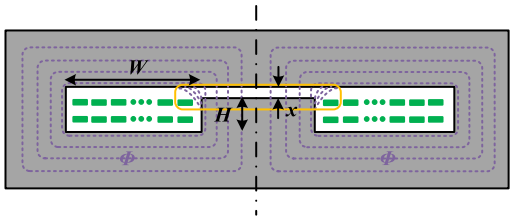

Fig. 3. Magnetic flux distribution considering the fringing effect.

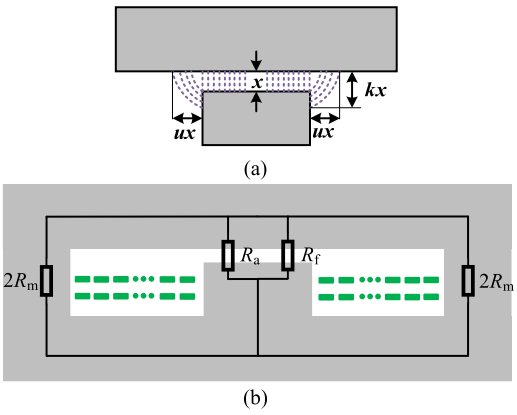

Fig. 4. Magnetic reluctance model of the undetermined coefficient method.

factor method (Method B-1). As described in [13], since the fringing effect will make the inductance value larger, it is a simple and effective way to directly increase the influence factor F based on the ideal calculation method in Section II-A. Influence factor F can be expressed as follows:

$$F = 1 + \frac{x}{\sqrt{D \cdot E}} \cdot \ln \frac{2 \cdot H}{x}. \tag{6}$$

By introducing the influence factor F, the modified inductance expression L_{fring1} is given as follows:

$$L_{\text{fring1}} = F \cdot \frac{N^2}{R_m + R_a}. \tag{7}$$

2) Undetermined Coefficient Method (Method B-2): The second modified method considering the fringing effect is called the undetermined coefficient method (Method B-2). As shown in Fig. 4(a), it is described in [14] that the existence of the fringing effect will lead to the change of the equivalent sectional area and the equivalent length. u and k are defined as the coefficients of the change for air gap area and length. Then, the fringing magnetic reluctance, which is parallel with the air gap magnetic reluctance, is introduced to show the influence of the fringing effect, as shown in Fig. 4(b). The fringing magnetic reluctance R_f is expressed as follows:

$$R_f = \frac{l_f}{\mu_a \cdot A_f} = \frac{k \cdot x}{\mu_a \cdot [(D + u \cdot x) \cdot (E + u \cdot x) - D \cdot E]} \tag{8}$$

where u and k are the expansion coefficients of the fringing magnetic flux. It is found that the increase of the magnetic flux radius is approximately equal to the length of the air gap; thus, the u and k parameters should both be 1 according to Kazimierczuk and Sekiya [14]. Therefore, the modified inductance expression

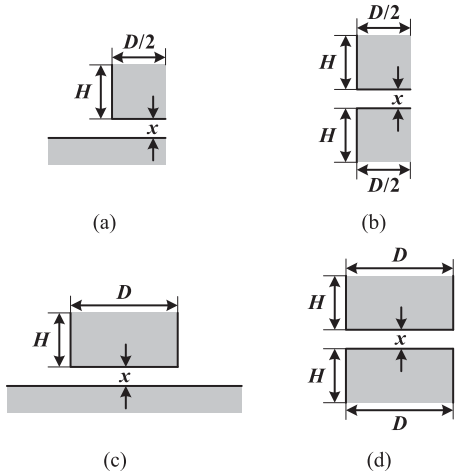

Fig. 5. Four basic geometric configurations. (a) Corner-face configuration. (b) Corner–corner configuration. (c) Pillar-face configuration. (d) Pillar–pillar configuration.

L_{fring2} using the second undetermined coefficient method is obtained as follows:

$$L_{\text{fring2}} = \frac{N^2}{R_m + R_a // R_f}. \tag{9}$$

3) Schwarz–Christoffel Transformation Method (Method B-3): The third modified method considering the fringing effect is the Schwarz–Christoffel transformation method (Method B-3) [16]. Four basic geometric configurations are proposed, as shown in Fig. 5. They can be used as the stepping stones in calculating the air gap magnetic reluctance considering the fringing effect.

For the planar EI core structures in this article, the pillar-face basic geometry, as shown in Fig. 5(c), is used for the magnetic reluctance calculation of the air gap. The modified air gap magnetic reluctance is described as $R_{a\text{-fring}}$

$$R_{a-\text{fring}} = \frac{1}{\mu_a \cdot \left(\frac{D}{x} + \frac{4}{\pi} \cdot \left(1 + \ln\left(\frac{\pi \cdot H}{4 \cdot x}\right)\right)\right) \cdot E}. \tag{10}$$

Therefore, the modified inductance expression L_{fring3} using the third Schwarz–Christoffel transformation method is obtained as follows:

$$L_{\text{fring3}} = \frac{N^2}{R_m + R_{a-\text{fring}}}. \tag{11}$$

The above three methods can be all employed for the correction of the inductance calculation when the fringing effect is taken into account.

III. Inductance Calculation Methods Considering Window Effect in a Planar Core

As illustrated in Section II-A and B, for typical magnetics with Litz wires, magnetic flux is almost all closed in the magnetic cores, while a little flux diffuses around the air gap, as shown in Fig. 6(a). However, for planar magnetics with PCB winding, there is a significant part of the flux diffusing in the magnetic core windows, as shown in Fig. 6(b). This is because the magnetic

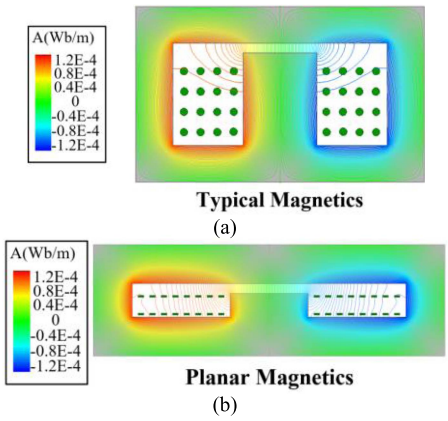

Fig. 6. FEA simulation comparison of the flux distribution for different magnetics. (a) Typical magnetics. (b) Planar magnetics.

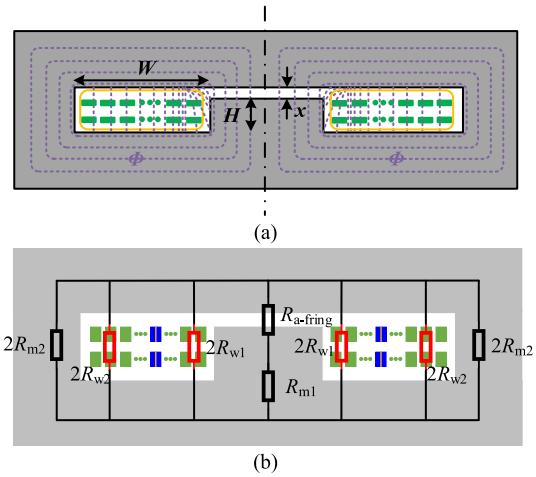

Fig. 7. Proposed calculation method considering both the fringing effect and the window effect. (a) Flux distribution. (b) Magnetic reluctance model.

reluctance of the core window becomes too small to be ignored as the magnetics are developing toward planarization. This phenomenon is defined as the "window effect" for planarized magnetic cores in this article. Due to the intensification of the window effect, there are more closed loops for magnetic flux. Hence, for the inductance calculation methods of the planar inductors, the methods in Section II-A and B are not accurate anymore. To improve the accuracy of the existing inductance calculation methods, a new method considering the window effect is proposed and described in detail as follows.

Still taking the planar EI core structure with the air gap on its middle winding column as an example, the flux distribution and its simplified magnetic reluctance model are shown in Fig. 7(a) and (b). The Schwarz–Christoffel transformation method is used to represent the influence of the fringing effect. In Fig. 7, $R_{a\text{-fring}}$ is the modified magnetic reluctance of the air gap, R_{w1} and R_{w2} are the magnetic reluctances of the core window, and R_{m1} and R_{m2} represent the magnetic reluctances of the magnetic cores. Two-layer PCB-winding structure is employed for the planar EI core. There are n turns of one layer and the turn marked by blue is the ith turn (n is the natural number and $1 \leq i \leq n$).

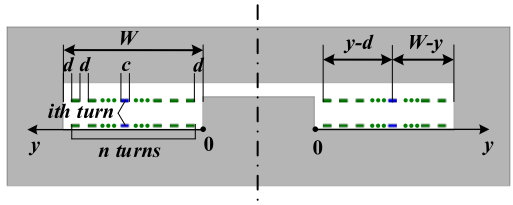

Fig. 8. Key dimension parameters of the windings.

For the planar magnetic cores considering both the fringing effect and the window effect, it is also suggested to calculate the total inductance value based on the lumped magnetic reluctance model. However, since the air gap is only above the middle winding column, the distribution of the magnetic flux is not uniform in the core window. Hence, lumping the window magnetic reluctances into a single reluctance cannot show this feature. The infinitesimal element method is combined into the proposed calculation method. The winding marked by orange is the current infinitesimal element of the ith turn.

As shown in Fig. 8, key dimension parameters of the PCB-winding structures are defined as follows: c is the width of one turn winding and d is the space between windings and windings or the magnetic core. Hence, $W = n * c + (n + 1) * d$. In addition, y is defined as the horizontal distance between the core window edge and the selected current element. $y - d$ means the horizontal distance between the current element and the PCB-winding edge close to the air gap. $W - y$ means the horizontal distance between the current element and the core-side leg edge. The definition range of y is d to $W - d$. To simplify the analysis, two assumptions are made: First, the window effect is decoupled from the fringing effect. It means the window flux vertically passes through the PCB winding and then is closed by the core. The fringing flux only exists around the air gap. Second, the magnetic lines of the core window are closed vertically.

For the two-layer n turns PCB-winding structures, the magnetic reluctances corresponding to the flux generated by each turn are different from each other. Hence, it is appropriate to solve the problem through the differential element method. Each turn of winding shall be calculated and solved, respectively. Furthermore, for the ith turn winding, the calculation methods for various magnetic reluctances, as shown in Fig. 7(b), are the key points for the accuracy of the inductance value. The detailed calculation process is given as follows.

1) Magnetic reluctance of the air gap
As illustrated in the previous sections, to describe the influence of the fringing effect, the air gap magnetic reluctance is modified as $R_{a\text{-fring}}$ using the third correction method

$$R_{a-\text{fring}} = \frac{1}{\mu_a \cdot \left(\frac{D}{x} + \frac{4}{\pi} \cdot \left(1 + \ln\left(\frac{\pi \cdot H}{4 \cdot x}\right)\right)\right) \cdot E}. \quad (12)$$

2) Magnetic reluctance of the magnetic cores
R_{m1} and R_{m2} represent the different magnetic reluctances of the inner and outer core flux paths for each current element, respectively. Their expressions are as follows if the nonlinear characteristics of the core material are not

considered:

$$\begin{cases} R_{m1}(y) = \frac{H+2\cdot D+2y}{\mu_m \cdot D \cdot E} \\ R_{m2}(y) = \frac{H+x+2\cdot D+W-2y}{\mu_m \cdot D \cdot E}. \end{cases} \tag{13}$$

3) Magnetic reluctance of the core window
The magnetic reluctances of the core window are described as R_{w1} and R_{w2}. The main difference between R_{w1} and R_{w2} is that their corresponding horizontal window widths are different from each other. One is $y - d$ and the other is $W - y$. Their expressions are as follows:

$$\begin{cases} R_{w1}(y) = \frac{H+x}{\mu_a \cdot (y-d) \cdot E} \\ R_{w2}(y) = \frac{H+x}{\mu_a \cdot (W-y) \cdot E}. \end{cases} \tag{14}$$

It should be mentioned that (13) and (14) are the functions of y because y varies from different winding current elements. In addition, the denominator of R_{w1} has a $(y - d)$ term instead of y term because the flux distribution of the area from the middle winding column edge to the winding (corresponding to the area of $y = 0–d$) is mainly influenced by the fringing effect, which has been considered in (12). The denominator of R_{w2} has a $(W - y)$ term because there are no gaps on the side legs for this core structure.

For each current element of the ith turn of one layer, as shown in Fig. 8, their positions of MMF vary from each other. Hence, the total magnetic reluctance $R_i(i)$ for the ith turn is derived by integrating its horizontal distance range based on the (12)–(14)

$$R_i(i) = \frac{\int_{i\cdot d+(i-1)\cdot c}^{i\cdot d+i\cdot c} \left[\frac{\left(R_{a-\text{fring}}+R_{m1}(y)\right)\cdot R_{w1}(y)}{R_{a-\text{fring}}+R_{m1}(y)+R_{w1}(y)} + \frac{R_{m2}(y)\cdot R_{w2}(y)}{R_{m2}(y)+R_{w2}(y)} \right] dy}{c}. \tag{15}$$

The equivalent window magnetic reluctances are related to the boundaries of the numerical computation of the integral in (15). Then, for n turns one-layer winding structure, the average inductance R_{average} of each turn can be expressed as follows:

$$R_{\text{average}} = \frac{\sum_{i=1}^{n} R_i\,(i)}{n}. \tag{16}$$

Thus, the improved calculated inductance L_{total} for the two-layer planar EI core structure is given as follows:

$$L_{\text{total}} = \frac{(2\cdot n)^2}{R_{\text{average}}}. \tag{17}$$

It should be mentioned that the proposed method considering the window effect can also be applied to the typical inductors with EE or EI core structures. However, because the height of the typical core window is high, the magnetic reluctance of the core window is so large that the window effect is not notable. The critical factor for whether to consider the window effect is the ratio of window flux to air gap flux. In this article, it is suggested that the window effect should be considered when $R_{m1}(W)$ is greater than one-tenth of $R_{a\text{-fring}}$ for simplification. It is worth noting that one-tenth is only the recommended value, which ought to be smaller for occasions with higher inductance accuracy requirements.

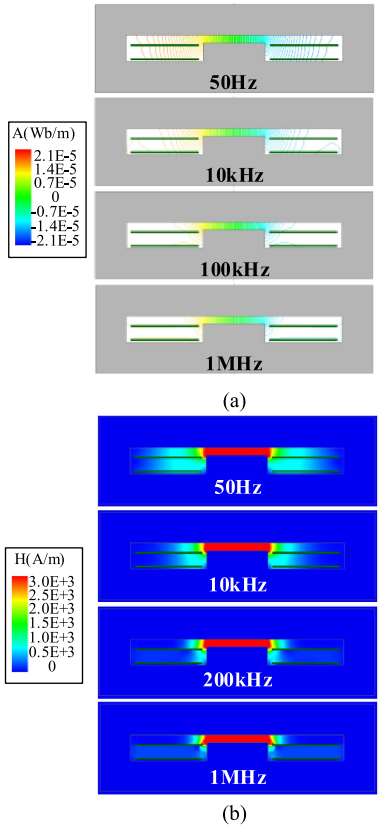

Fig. 9. Schematic diagram of magnetic flux distribution of air and winding. (a) Magnetic field lines distribution. (b) Magnetic field intensity distribution.

IV. Inductance Calculation Considering the Shielding Effect of PCB Windings

For the proposed inductance calculation method in Section II, the PCB windings are considered as the air. This assumption will no longer be applicable as the switching frequency becomes higher. Since copper is a good conductor, there will be an eddy current induced in the winding, which will offset the original magnetic flux. This phenomenon is called the shielding effect of winding in this article. As shown in Fig. 9(a), magnetic field line distributions of different switching frequencies with the range of 50 Hz–1 MHz are presented based on the FEA simulation software. Obviously, with the increase in switching frequency, the shielding effect of the PCB winding is more and more notable. Less magnetic flux crosses through the winding, which means that the equivalent magnetic reluctance of the core window becomes larger and the corresponding inductance gets smaller. The above-mentioned analysis is also verified by the distribution of the H field, as shown in Fig. 9(b). The magnetic field intensity of the core window is also decreasing with the increase of switching frequency. On this basis, permeability coefficient p is introduced to represent the change of equivalent magnetic reluctance of the window. The definition of the permeability coefficient p is based on the concept of the penetration depth. Since the amplitude of the magnetic field intensity will attenuate along the depth of the conductor, penetration depth is usually utilized to describe the distance that the amplitude of a field quantity attenuates to $1/e$

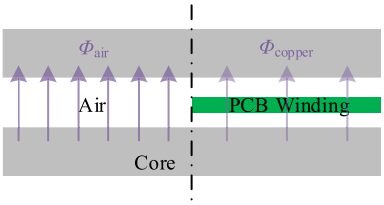

Fig. 10. Schematic diagram of magnetic flux distribution of air and winding.

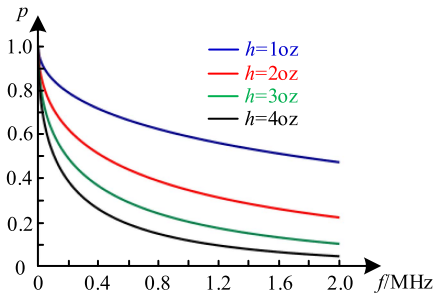

Fig. 11. Relationship between the permeability coefficient and switching frequency along with copper thickness.

of its surface value according to Wheeler [20]. Hence, as shown in Fig. 10, the permeability coefficient p represents the ratio of magnetic flux through winding to that of not through winding

$$p = \frac{\Phi_{\text{copper}}}{\Phi_{\text{air}}} = e^{-h\cdot\sqrt{\gamma\cdot\mu_c\cdot\pi\cdot f}} \tag{18}$$

where h is the copper thickness, while f is the switching frequency. γ represents the conductivity and μ_c represents the permeability of copper, which is the same as that of the air. Fig. 11 shows the relationship between the permeability coefficient and switching frequency along with copper thickness. Since the expression of p is concise and covers a complete range of influencing factors, it is chosen as the coefficient to represent the influence of switching frequency. Based on the above analysis, the magnetic reluctance of the core window is modified as follows:

$$\begin{cases} R_{w1-\text{improved}}(i,y) = \frac{H+x}{\mu_a\cdot((i-1)\cdot d+(y-i\cdot d)\cdot p)\cdot E} \\ R_{w2-\text{improved}}(i,y) = \frac{H+x}{\mu_a\cdot((n-i+1)\cdot d+(n\cdot c+i\cdot d-y)\cdot p)\cdot E}. \end{cases} \tag{19}$$

The calculation methods of other magnetic reluctances are the same as before. Then, the improved calculation method considering the shielding effect of the winding is obtained.

In a word, when considering the window effect, it means there is a little magnetic flux closed by the core window. This flux part will go through the PCB winding. However, for low-frequency magnetics, there will be no eddy current induced in the PCB winding. Hence, the magnetic flux distribution of the core window will not change if other windings are considered as the air during the analysis process. However, for high-frequency magnetics, the shielding effect of PCB winding ought to be taken into account. The permeability coefficient p commendably shows the effect of the switching frequency on inductance values.

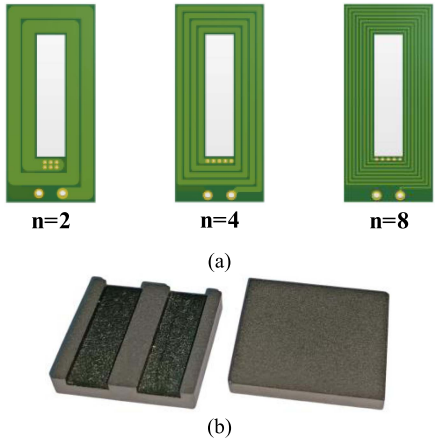

Fig. 12. Measured planar EI cores with different winding turns. (a) Different PCB-winding structures with different turns. (b) Planar EI core structure.

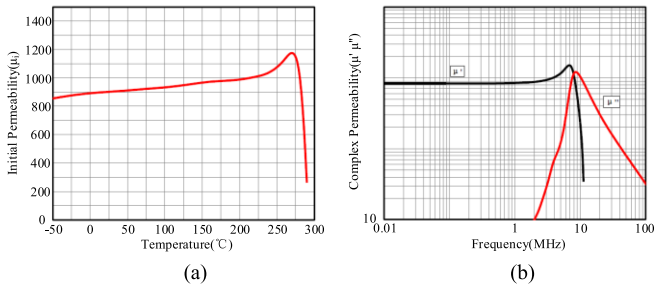

Fig. 13. Permeability of the DMR51W. (a) Relationship between the permeability and the temperature. (b) Relationship between the permeability and frequency.

TABLE I
DETAILS OF THE SELECTED CORE MATERIAL

Parameter	Value
Model number	DMR51W
Manufacturer	DMEGC.
Initial permeability	900*μ_a
Saturation magnetic flux density	500mT
Residual magnetic flux density	120mT
Coercive force	45A/m

V. SIMULATION AND EXPERIMENTAL RESULTS

This section presents the calculation, simulation, and experimental results of multiple inductors using planar EI core structures with different air gaps, switching frequency, and winding turns. The structures of multiple planar EI cores are shown in Fig. 12. Two layers PCB-winding structures are employed. Each turn of the winding is connected in series. The terminals/pins of the connection have little influence on the inductance value because they are parallel to the magnetic lines of force. The planar EI core structure is provided by Hengdian Group Dongci Company, Ltd. Its material model number is DMR51W and other detailed parameters are shown in Table I [21]. Its permeability is around $900 * \mu_a$ and its relationships with the temperature and the switching frequency are shown in Fig. 13(a) and (b). It is shown that, when the room temperature is 25 °C and the switching frequency does not exceed 1 MHz, its permeability is

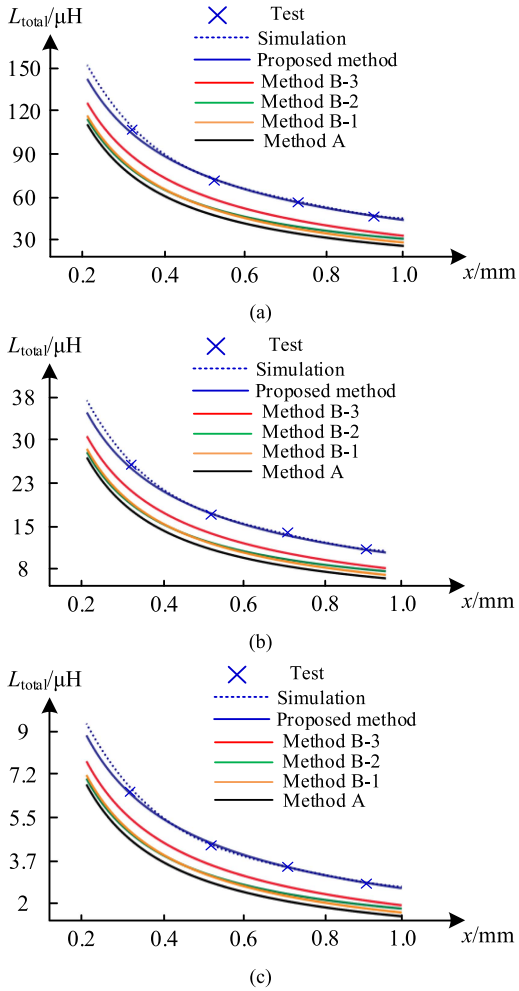

Fig. 14. Influence of the window effect on inductance and method comparison. (a) $n = 8$ per layer. (b) $n = 4$ per layer. (c) $n = 2$ per layer.

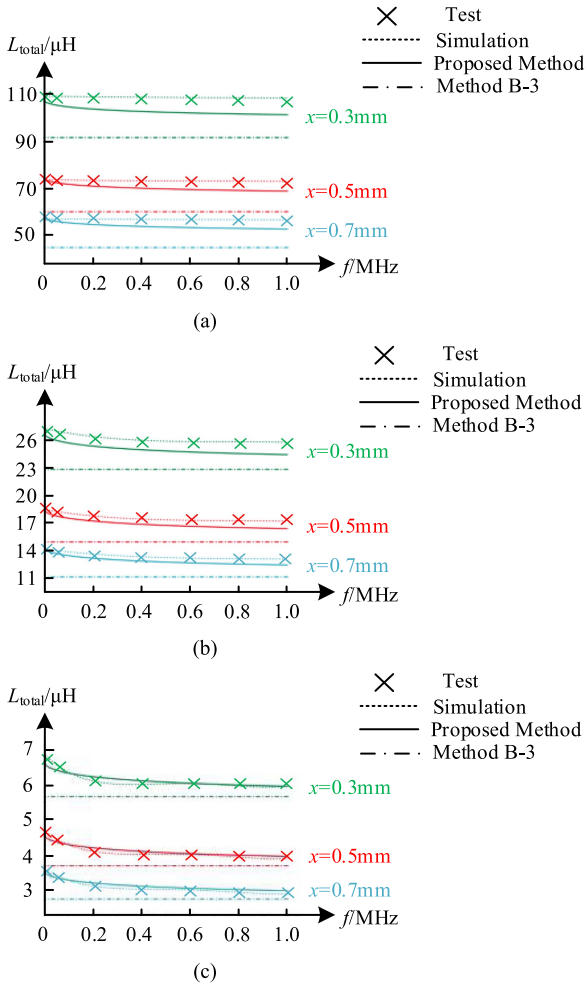

Fig. 15. Influence of the switching frequency on inductance and method comparison. (a) $n = 8$ per layer. (b) $n = 4$ per layer. (c) $n = 2$ per layer.

almost constant. Therefore, for the final measured planar magnetics, fixed dimension parameters are $D = 4$ mm, $E = 20$ mm, $H = 1.2$ mm, $d = 0.3$ mm, and $h = 3$ oz; free dimension parameters are $x = 0.2$–1 mm, $n = 2, 4, 8$, and $f = 50$ Hz–1 MHz.

According to the analysis in Sections II and III, the traditional inductance calculation methods are not suitable for planarized magnetic cores. Hence, the improved calculation method is proposed. The differences between them are analyzed in detail through simulation and experimental results as follows.

A. Influence of the Core Planarization

The influence of the core planarization is reflected in the introduction of the window magnetic reluctances (R_{w1} and R_{w2}). The ideal calculation method and the other three modified calculation methods considering the fringing effect are all taken as comparisons. In this section, the switching frequency is set at the power frequency of 50 Hz and the simulation method is three-dimensional FEA. The calculation, simulation, and the experimental results with different winding turns and air gaps are shown in Fig. 14(a), (b), and (c), respectively. It can be found that, when only the fringing effect is added to the calculation, the inductance values obtained by three modified calculation methods in Section II-B are all larger the those obtained by the ideal calculation method. This is consistent with the previous theoretical analysis. However, no matter which calculation method is considering the fringing effect, the calculation results are still lower than the experimental results. Therefore, based on the Schwarz–Christoffel transformation method, the new calculation method conserving the window effect is improved and proposed. Obviously, as the window effect is taken into account, the inductance calculation results further increase, and the differences between the calculation results, simulation results, and experimental results can be almost ignored.

B. Influence of the Switching Frequency

The influence of the switching frequency is reflected in the introduction of the permeability coefficient p. Due to the shielding effect of the PCB winding, the inductance values become lower as the switching frequency is approaching higher. As shown in Fig. 15(a)–(c), during the full range of the air gap distances, the calculation results are consistent with the theoretical analysis. However, according to the definition of the permeability,

with the increase of the switching frequency, the amplitude of the inductance value decrease is not linear. In addition, among the low-frequency band (0–200 kHz), the inductance values decrease significantly, while in the high-frequency band (200 kHz–1 MHz), the inductance values are almost unchanged.

The calculation results, simulation results, and the experimental results of different core structures with various switching frequencies (0–1 MHz) are shown in Fig. 15(a)–(c). The calculation results obtained by the method proposed in this article are closer to the simulation and experimental results than those obtained by the Schwarz–Christoffel transformation method. In addition, the influence of the switching frequency on the inductance can also be reflected by the proposed calculation method. It should be mentioned that, as the turn windings increase, the error between the calculated results and the experimental results also increases. This is because the number of gaps between windings is increasing, and then the shielding effect of the winding is weakened to some extent. In general, the shielding effect of the high-frequency winding is well displayed by the introduction of the permeability coefficient p.

VI. Conclusion

The window effect of PCB-winding planarized inductors is analyzed in detail. It is found that, due to the lower height and planarized structure, the core window of a planarized inductor can be regarded as a big air gap, which has a great impact on the real inductance of the inductor and cannot be ignored anymore. In this article, the core window magnetic reluctances are considered for the inductance calculation model. In addition, a new permeability coefficient is introduced to represent the shielding effect of the PCB windings on high-frequency magnetic flux and further improve the calculation accuracy.

To verify the accuracy of the proposed inductance calculation model, the inductance of various planar EI cores with different winding turns, switching frequencies, and air gaps is verified by both FEA simulation results and experimental results, which verify that the proposed model is more accurate than previous inductance calculation methods.

Acknowledgment

The authors would like to thank Hengdian Group Dongci Company, Ltd., for providing planar magnetic cores for the research in this article.

References

[1] M. de Rooij and Q. Laidebeur, "Meeting the power and magnetic design challenges of ultra-thin, high-power density 48 V DC-DC converters for ultra-thin computing applications," *IEEE Power Electron. Mag.*, vol. 8, no. 3, pp. 30–36, Sep. 2021.

[2] M. Hua, J. Chen, G. Xu, and H. Wu, "Ultra-thin coupled inductor for a GaN-based CRM buck converter," in *Proc. IEEE Workshop Wide Bandgap Power Devices Appl. Asia*, 2021, pp. 138–142.

[3] J. Millán, P. Godignon, X. Perpiñà, A. Pérez-Tomás, and J. Rebollo, "A survey of wide bandgap power semiconductor devices," *IEEE Trans. Power Electron.*, vol. 29, no. 5, pp. 2155–2163, May 2014.

[4] E. A. Jones, F. F. Wang, and D. Costinett, "Review of commercial GaN power devices and GaN-based converter design challenges," *IEEE J. Emerg. Sel. Topics Power Electron.*, vol. 4, no. 3, pp. 707–719, Sep. 2016.

[5] Y. Liu, Y. Song, D. Hu, Y. Li, Z. Zhang, and H. Wu, "Overview of planar magnetics for high-frequency resonant converters," *Chin. J. Elect. Eng.*, vol. 8, no. 4, pp. 61–78, Dec. 2022.

[6] M. Chen, M. Araghchini, K. K. Afridi, J. H. Lang, C. R. Sullivan, and D. J. Perreault, "A systematic approach to modeling impedances and current distribution in planar magnetics," *IEEE Trans. Power Electron.*, vol. 31, no. 1, pp. 560–580, Jan. 2016.

[7] X. Huang, F. C. Lee, Q. Li, and W. Du, "High-frequency high-efficiency GaN-based interleaved CRM bidirectional buck/boost converter with inverse coupled inductor," *IEEE Trans. Power Electron.*, vol. 31, no. 6, pp. 4343–4352, Jun. 2016.

[8] J. Chen, L. He, and B. Cheng, "Optimized parameter design method for wide-input-voltage LLC converter with frequency-based self-adapted magnetizing inductance," in *Proc. IEEE Int. Symp. Predictive Control Elect. Drives Power Electron.*, 2019, pp. 1–4.

[9] R. Shafaei, M. C. G. Perez, and M. Ordonez, "Planar transformers in LLC resonant converters: High-frequency fringing losses modeling," *IEEE Trans. Power Electron.*, vol. 35, no. 9, pp. 9632–9649, Sep. 2020.

[10] H. Xu, H. Kamada, S. Nomura, H. Chikaraishi, H. Tsutsui, and T. Isobe, "A simple calculation method for center magnetic flux density of a magnetic core electromagnet with a wide air gap," *IEEE Trans. Appl. Supercond.*, vol. 32, no. 6, Sep. 2022, Art. no. 4900606.

[11] Z. Ouyang and M. A. E. Andersen, "Overview of planar magnetic technology—Fundamental properties," *IEEE Trans. Power Electron.*, vol. 29, no. 9, pp. 4888–4900, Sep. 2014.

[12] S. Mukherjee, Y. Gao, and D. Maksimović, "Reduction of AC winding losses due to fringing-field effects in high-frequency inductors with orthogonal air gaps," *IEEE Trans. Power Electron.*, vol. 36, no. 1, pp. 815–828, Jan. 2021.

[13] C. W. T. McLyman, *Transformer and Inductor Design Handbook*. New York, NY, USA: Taylor & Francis, 2004, pp. 370–372.

[14] M. K. Kazimierczuk and H. Sekiya, "Design of AC resonant inductors using area product method," in *Proc. IEEE Energy Convers. Congr. Expo.*, 2009, pp. 994–1001.

[15] Z. Yang, H. Suryanarayana, and F. Wang, "An improved design method for gapped inductors considering fringing effect," in *Proc. IEEE Appl. Power Electron. Conf. Expo.*, 2019, pp. 1250–1256.

[16] A. Balakrishnan, W. T. Joines, and T. G. Wilson, "Air-gap reluctance and inductance calculations for magnetic circuits using a Schwarz-Christoffel transformation," *IEEE Trans. Power Electron.*, vol. 12, no. 4, pp. 654–663, Jul. 1997.

[17] J. Muhlethaler, J. W. Kolar, and A. Ecklebe, "A novel approach for 3D air gap reluctance calculations," in *Proc. 8th Int. Conf. Power Electron.-ECCE Asia*, 2011, pp. 446–452.

[18] M. Akbari, A. Rezaei-Zare, M. A. M. Cheema, and T. Kalicki, "Air gap inductance calculation for transformer transient model," *IEEE Trans. Power Del.*, vol. 36, no. 1, pp. 492–494, Feb. 2021.

[19] Y. Tian, Y. Li, and J. Liu, "Fringing field analytical calculation of high frequency planar magnetic components," *CPSS Trans. Power Electron. Appl.*, vol. 7, no. 3, pp. 251–258, Sep. 2022.

[20] H. A. Wheeler, "Formulas for the skin effect," *Proc. IRE*, vol. 30, no. 9, pp. 412–424, Sep. 1942.

[21] Hengdian Group Dongci Co., Ltd., "DMR51W datasheet," 2018. [Online]. Available: https://www.chinadmegc.com/product/1.html

Yue Liu was born in Jiangsu Province, China, in 1997. He received the B.S. degree in electrical engineering in 2019 from the Nanjing University of Aeronautics and Astronautics, Nanjing, China, where he is currently working toward the Ph.D. degree in electrical engineering.

His main research interests include magnetic integration, planar magnetics, and resonant converters.

Hongfei Wu (Senior Member, IEEE) received the B.S. and Ph.D. degrees in electrical engineering and power electronics and power drives from the Nanjing University of Aeronautics and Astronautics (NUAA), Nanjing, China, in 2008 and 2013, respectively.

Since 2013, he has been with the Faculty of Electrical Engineering, NUAA, and is currently a Professor with the College of Automation Engineering, NUAA. He has authored and coauthored more than 250 peer-reviewed papers published in journals and conference proceedings. He is the holder of more than 40 patents. His research interests include high-performance power converters, wide-band-gap device applications, and magnetic integration.

Dr. Wu was the recipient of the Best Associate Editor for Journal of Power Electronics (2018), the Outstanding Reviewer of IEEE Transactions on Power Electronics (2013 and 2022), the Changkong Scholar Award, and the Young Scholar Innovation Award of NUAA (2017). He serves as an Associate Editor for the *Journal of Power Electronics*, *CPSS Transactions on Power Electronics and Applications*, *Chinese Journal of Electrical Engineering*, and *Power Electronic Devices and Components*. He is the Guest Associate Editor for the IEEE JOURNAL OF EMERGING AND SELECTED TOPICS IN POWER ELECTRONICS.

Guosheng Ji (Member, IEEE) was born in Jiangsu Province, China, in 2001. He received the B.S. degree in electrical engineering in 2023 from the Nanjing University of Aeronautics and Astronautics (NUAA), Nanjing, China, where he is currently working toward the M.S. degree in electrical engineering.

His main research interests include magnetic integration and resonant converters.